MHD MODELLING OF METAL FLOW BARRIERS

Dagoberto S. Severo[(1)], Vanderlei Gusberti[(1)].

1) CAETE Engenharia, Rua Caeté 162, Porto Alegre RS– Brazil
caete@caetebr.com

Keywords: aluminium reduction cell, magnetohydrodynamics, CFD modelling, OPENFOAM, metal flow barrier.

Abstract

In large scale aluminium reduction cells, the MHD metal pad flow is one of the most important factors influencing the cell current efficiency. As the cell current and size increase in new cell projects, the electromagnetic forces and velocities present in the metal pool become stronger. Irregular cathode surfaces and metal pad barriers are options to decrease the metal velocity and improve MHD stability by reducing the wave amplitude and growth rate.

One of the drawbacks of most studied structured cathodes is the difficulty to perform a satisfactory cathode cleaning procedure, which may favour sludge formation and potentially increasing cathode voltage drop. In the present work the shape of the barriers is designed in order to keep the cathode cleaning procedure possible. In addition, a large barrier at the central channel may help to avoid sludge formation due to alumina precipitation at that location.
A magnetohydrodynamic model was developed in OPENFOAM open source CFD code. The models were used to predict the improvement in MHD features for some different barrier designs.

Introduction

In aluminium electrolysis cells, the magnetohydrodynamic (MHD) strongly affects the cell operation efficiency [1]. Throughout the history, many cell design features have been proposed and used in order to improve the cell MHD behaviour, such as: busbar modifications, riser position modifications, collector bar copper inserts. As the cell size increased in the last decades, the metal pool area increased and there is more space for metal velocities and waves to develop.

One way that has been proposed back in the 80's (see [3] and [4]) to reduce metal pool velocities and metal waves is to place physical barriers on the cathode panel. In the referred patents, many barriers were installed under the anodes with the objective of reducing metal motion and wave formation. The central channel was left free from barriers. In another patent [5], barriers of a variety of shapes are claimed with the function of redirecting and improving the metal flow.

In another work [6], laboratory scaled cell experiments were performed using barriers in the metal pad and the results are compared with numerical models. It found that the barriers have the ability to improve the MHD stability threshold.

A central channel barrier is disclosed in [7], where the barrier is made of a bath attack resistive material. The barrier surpasses the interface level, fully isolating the metal pad in distinct volumes. In the referred patent, it is claimed that the interface MHD wave would present smaller amplitudes and shorter periods in the separated metal volumes, improving MHD instability.

Structured cathodes [10] also produce a similar effect of metal barriers; the structures function as a collection of small barriers. Some works report important gains in energy efficiency when using structured cathodes, for example, Naixiang et al. [8] claim that they improved the cell energy efficiency by 1.0 kWh/ kg Al with structured cathodes.

The main advantage of the barriers over the structured cathode panel is the possibility to maintain a planar cathode below the anode. The cathode top cleaning procedure is then feasible using the same equipment of traditional cells, usually called "bath scoop". Pieces of carbon, cover material and sludge need to be taken out from the cell periodically in order to obtain good cell operation. In the literature, no description has been found of how a structured cathode would be cleaned.

MHD Models in Openfoam

In a previous work, the authors developed MHD simulations using CFD commercial packages [2]. In the present article a similar methodology was developed in an open source CFD code Openfoam. The magnetic fields and Lorentz forces were previously obtained in the same way as presented in [2]. A special routine for importing the electromagnetic fields was developed by CAETE. The metal and bath are immiscible fluids; the Openfoam models use the VOF method (volume of fluid) to separate the liquid phases.

In the routine implemented in Openfoam, the total electromagnetic force "F_{EM}" is the source term of the momentum equation for fluids, also called the Navier-Stokes equation. The electromagnetic forces are given by Equation (1), which includes the flow-induced electrical current, $\sigma(\mathbf{v}\times\mathbf{B})$. The induced current is significant only in metal pool region due to its higher electrical conductivity.

$$\mathbf{F}_{EM} = \mathbf{J}\times\mathbf{B} + \sigma(\mathbf{v}\times\mathbf{B})\times\mathbf{B} \qquad (1)$$

Where **J** is the current density vector, **B** is the magnetic flux density vector, σ is electrical conductivity, **v** is the fluid velocity vector. Note that the forces are recalculated every iteration, because they are dependent on the calculated fluid velocities.

The first test for the Openfoam modeling system was to run the benchmark case proposed by Severo et al. in 2008 [9]. The Figure 1 presents the metal velocity vectors at the middle of the metal pad for the referred benchmark case. The pattern obtained is in agreement with the other results obtained by distinct softwares [9].

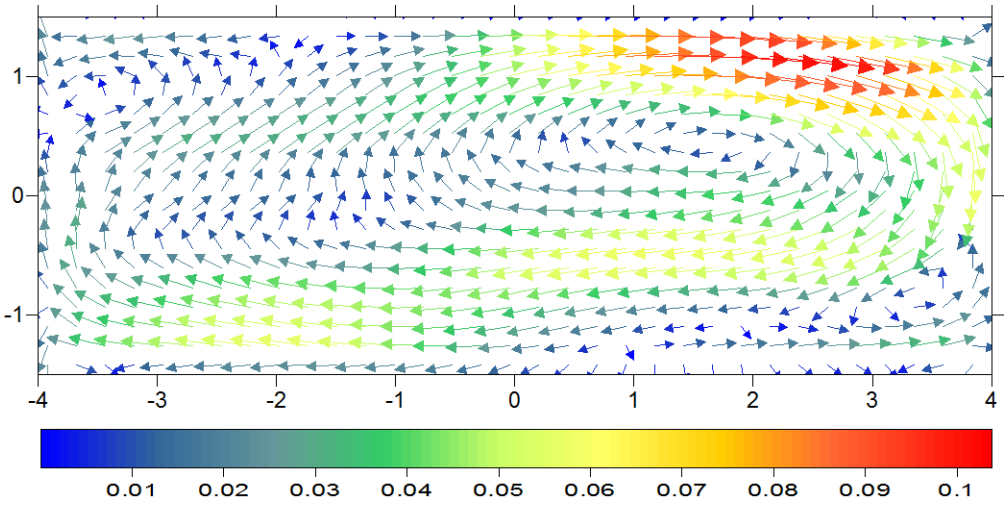

Figure 1: Metal flow at the middle of the metal pad for the benchmark case

In Figure 2 the metal/bath interface deformation obtained by the VOF method is shown. The interface shape is similar to other software results regarding the central elevation. It appears that the Openfoam 2 phases VOF result is closer to the 3 phase CFX result presented in [9].

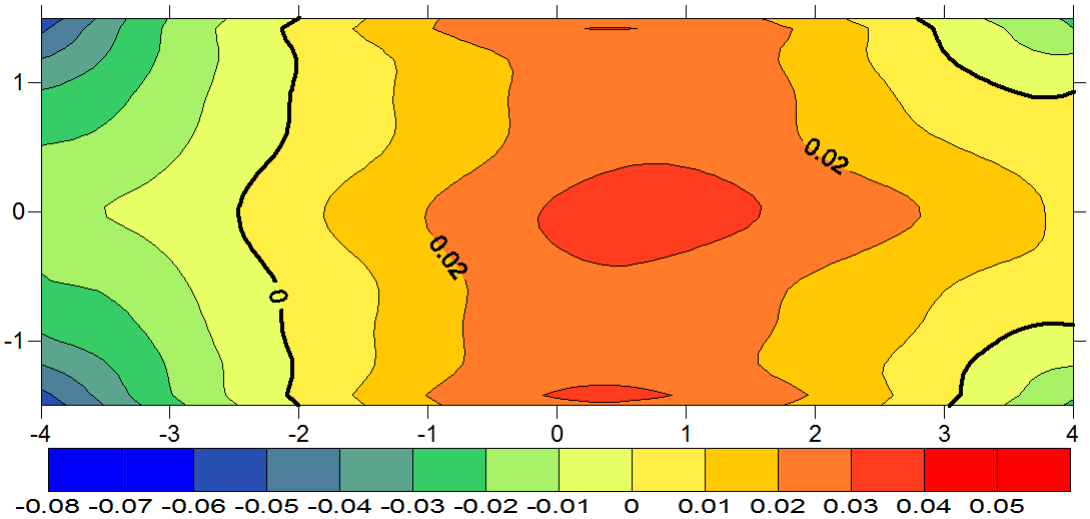

Figure 2: Metal/bath interface deformation of the benchmark case

Additionally, the interface profile on the longitudinal axis located at the center of the cell is shown is shown in Figure 3 compared with previous models [9]. The interface is inclined in the positive direction in good agreement between the software packages.

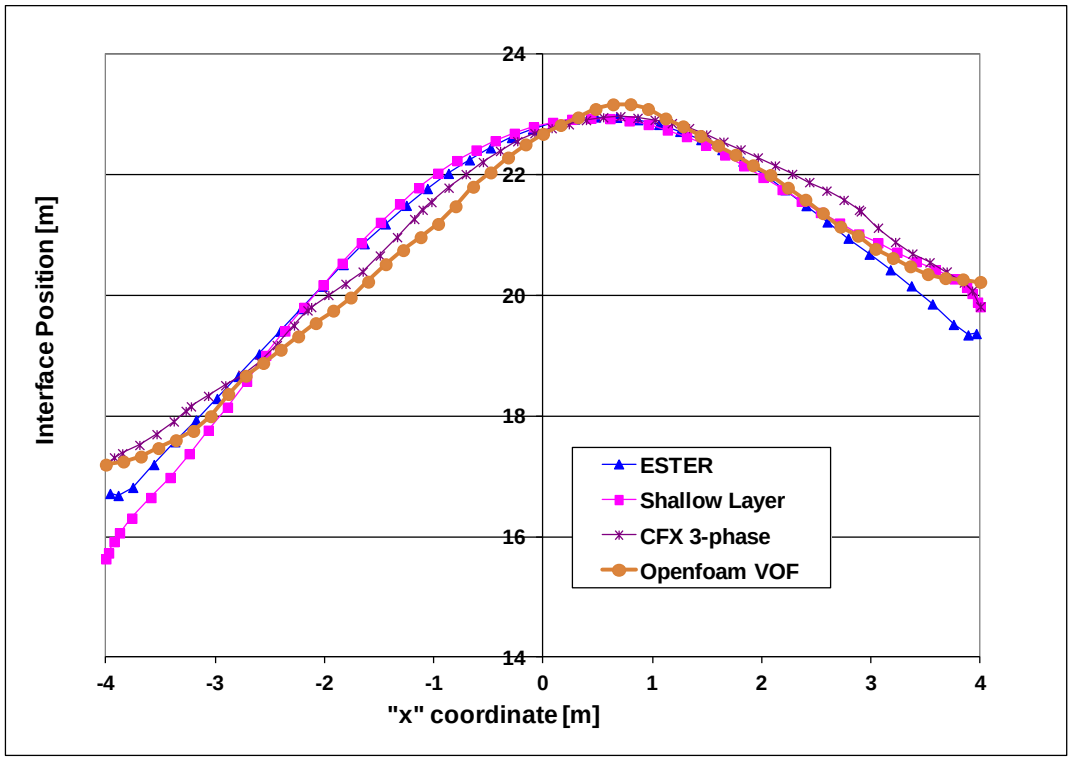

Figure 3: Comparison of calculated interface profiles for the benchmark case using Openfoam compared with other softwares [9]

Modelling of Cell MHD Using Barriers

MHD modelling of a structured cathode cell presenting rounded carbon protrusions compared with a traditional cell was presented in [11]. The cited model was done using Ansys and CFX commercial softwares. It was found that the protrusions reduce the average velocities of the metal pad.

In another work, MHD steady state model (using Ansys software packages) was used to show features of the metal and bath flow that are present when using cathode protrusions such as the vertical velocities present near a barrier or protrusions [12]. When flow barriers or protrusions are present in the cell, vertical velocities and vertical fluid circulations are produced. These fluid flow features are not evaluated when using shallow water method [13], [14]. This may be the reason why shallow water models do not show important gains in cell stability when using structured cathodes as discussed also in [15], in contradiction with the experiments performed in real cells [16].

Enhancing the friction at the bottom of the metal pad in shallow water models is a way to represent the structures on the cathode [17]. However, this approach may not be suitable to represent flow wave breaker barriers, because not only the high friction must be represented but also the vertical fluid velocity caused by the barrier has important influence on the wave behaviour. We believe that only by using a three-dimensional approach it is possible to properly evaluate the effects of cathode panel barriers and structures on the MHD cell behaviour.

A Reynolds P-19 side-by-side end riser cell, where magnetic fields [2] and metal velocities were modeled and validated by CAETE (Figure 4 and Figure 5), was chosen to perform MHD calculations and developments of the metal barriers.

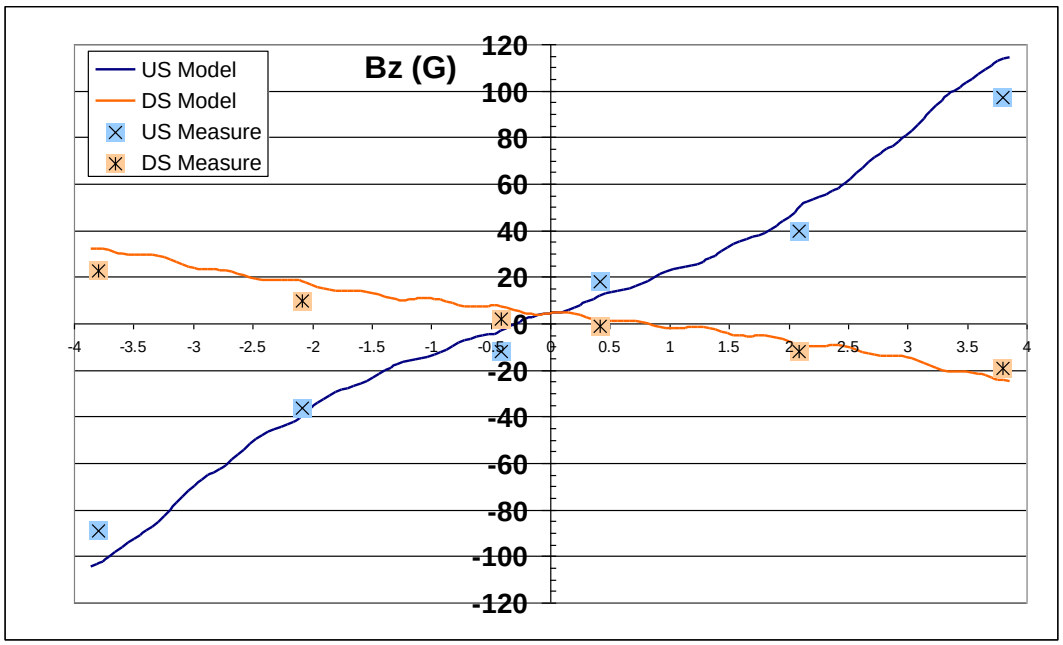

Figure 4: Vertical component of magnetic field (Bz), measurements versus model calculations

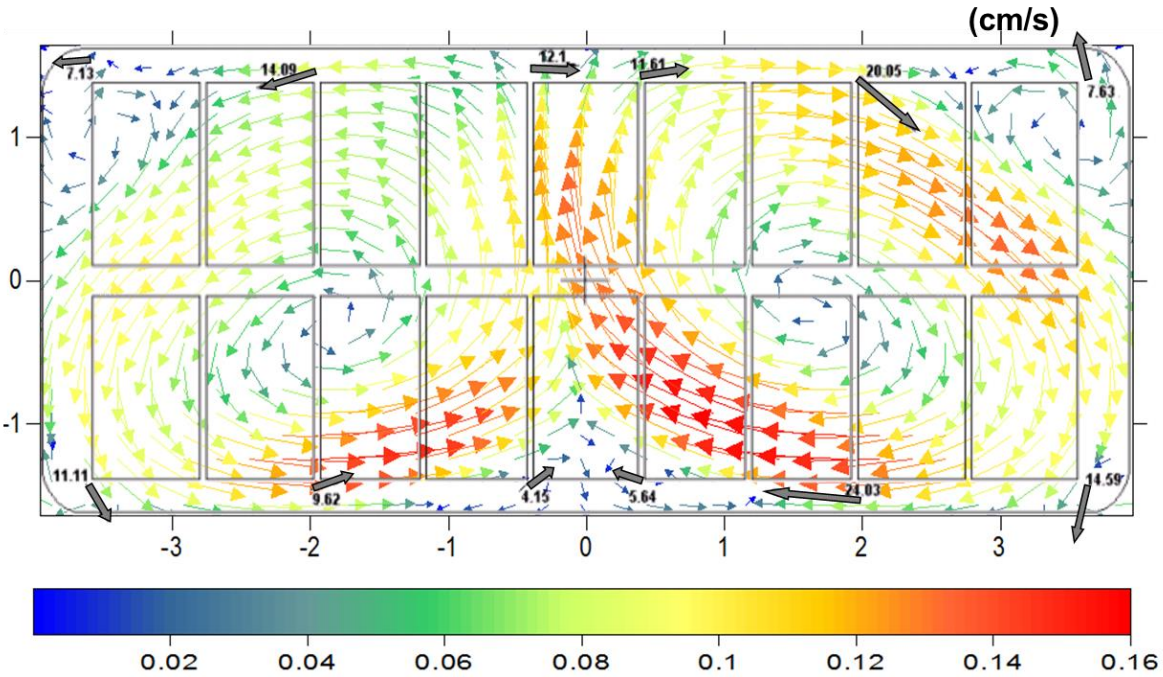

Figure 5: Metal velocities at the metal pool. (Horizontal plane at the meddle of metal height). Measurements versus model results obtained in Openfoam

The cell current is 168 kA, metal height is 245 mm, and the ACD is considered 50 mm in the models. The Figure 6 shows the central panel barrier disposition placed on the cathode panel.

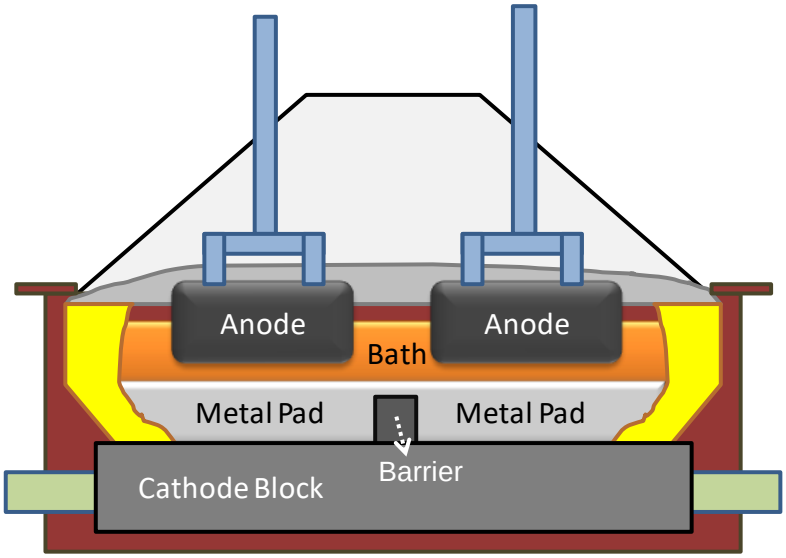

Figure 6: Schematic view of the central channel barrier in the cell. Vertical cut

In this work, four configurations of metal barriers (200 mm height, 200 mm width) are studied as well as a structured cathode case (structures are 100 mm high). The cases are presented in the Figure 7. The impact of such configurations on the metal flow and interface deformation is discussed. In opposition of the invention disclosed in [7], the barriers do not reach the bath level (45 mm lower in average). Therefore they don't need to be made of a bath attack resistive material.

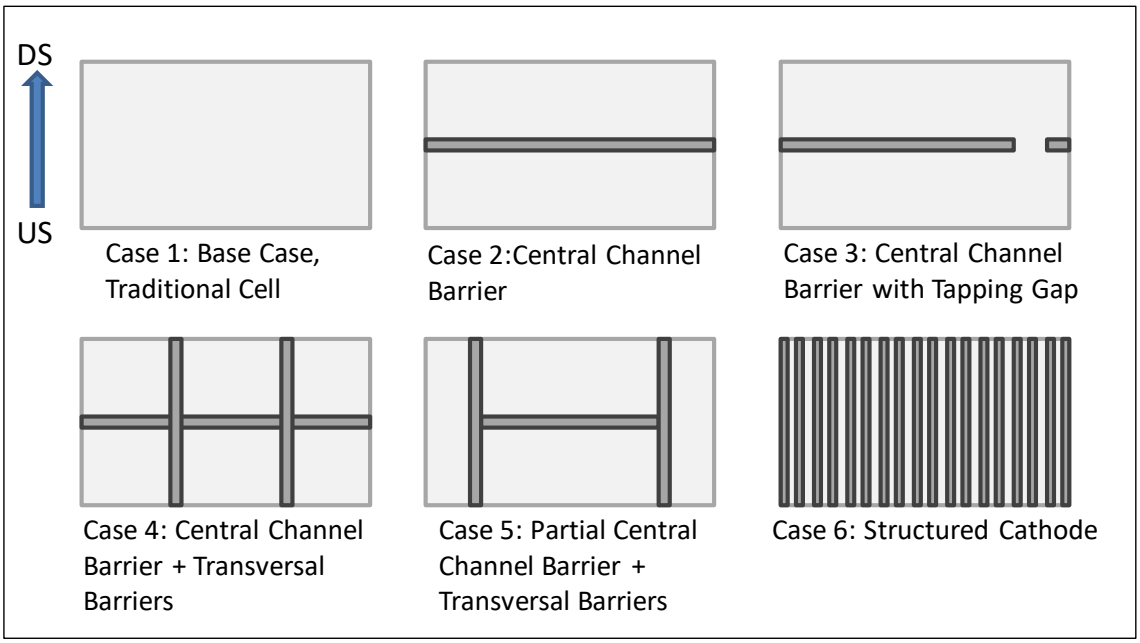

Figure 7: Case options for the MHD flow calculations of the barrier study. Schematic top view of barrier configurations and structured cathode.

In the Figure 8 metal flow velocities for the traditional cell without metal barriers are presented. Two strong metal pools are identified. Such metal velocity configuration is typical of side-by-side aluminium reduction cell of this size.

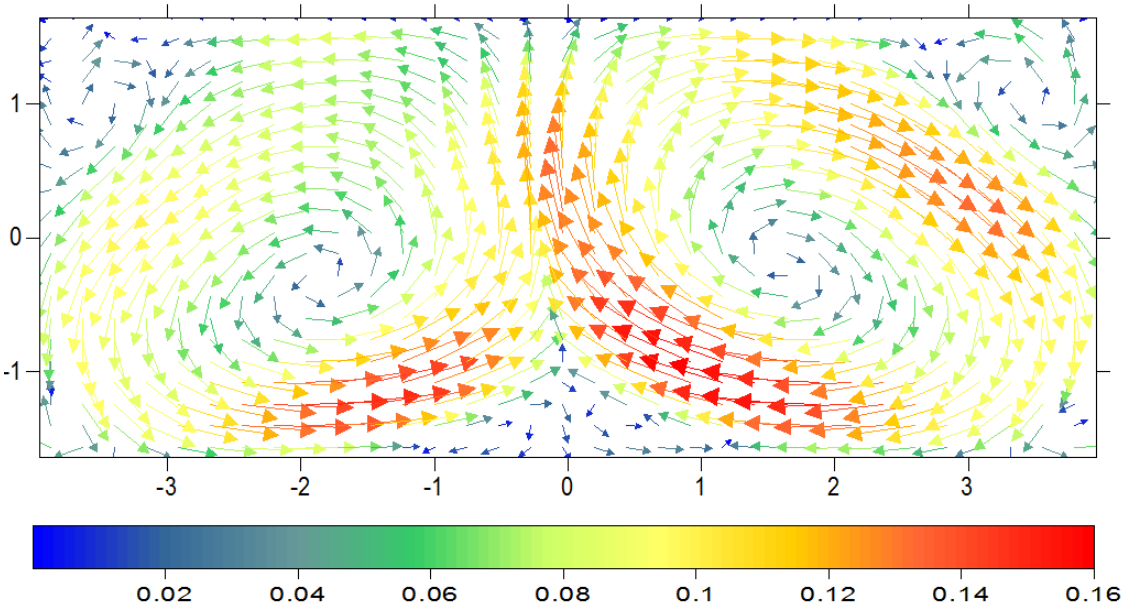

Figure 8: Metal velocities [m/s] calculated at the middle of the metal pad horizontal plane for case 1

The first approach to reduce the metal pool velocities is to place a barrier at the central channel. Such barrier would divide the pools in smaller recirculation pools at upstream and downstream. The Figure 9 presents the metal flow for the central barrier case of the studied cell.

In many cell designs the tapping of liquid aluminium is made at the central channel near the tapping end. In this type of the cell, the central barrier would need a gap for the crucible pipe placement. The Figure 10 presents the metal velocity vectors obtained when using the central channel barrier with the gap at the tapping end. In this case the decrease in the velocities is somewhat less efficient than the integral barrier, as expected. However the gain related to the traditional cell is still important.

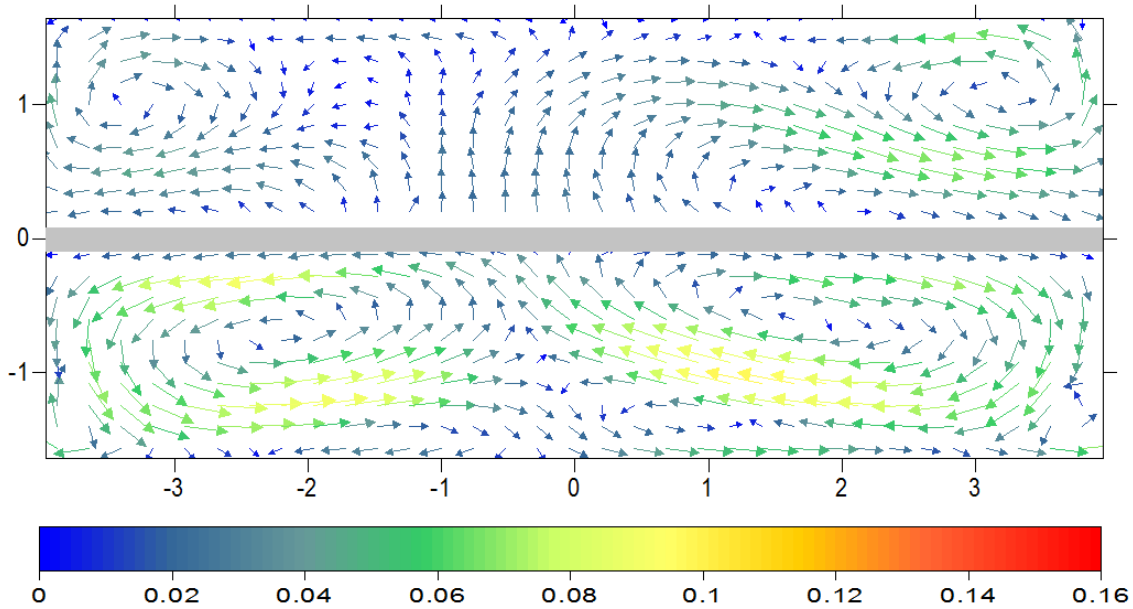

Figure 9: Metal velocities [m/s] calculated at the middle of the metal pad horizontal plane for case 2

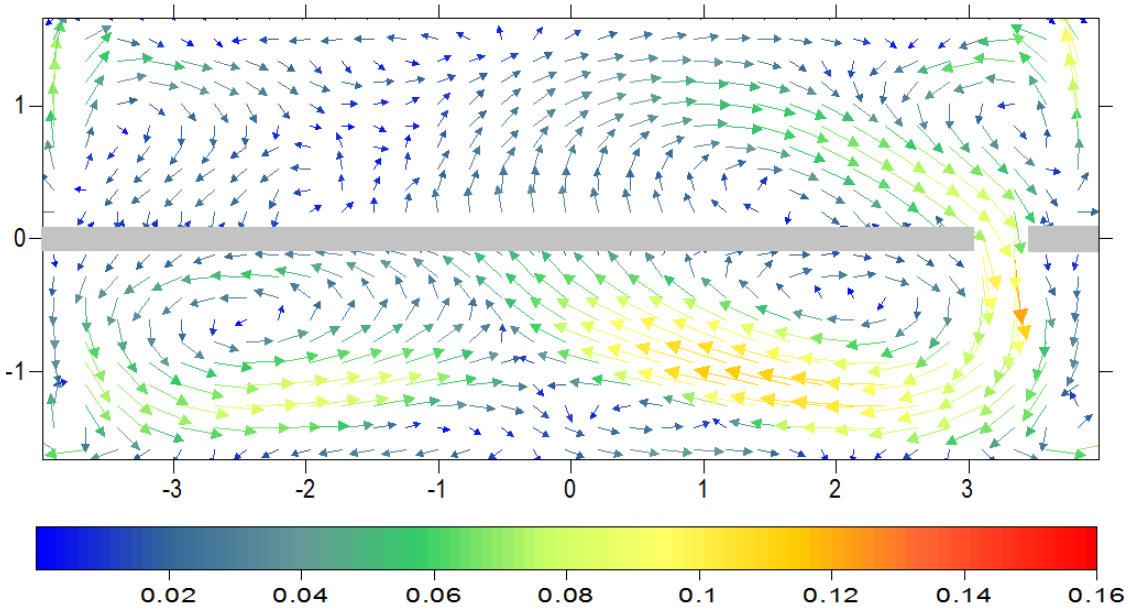

Figure 10 Metal velocities [m/s] calculated at the middle of the metal pad horizontal plane for case 3

Another option is to place barriers at the gaps between adjacent anodes. Such positioning still allow the cathode top cleaning with the "cavity scoop" during anode change in the way currently done in most cell technologies. In the Figure 11 two transversal barrier were placed in adidition to the central channel barrier. More velocity reduction is observed in this case.

In another variant seen in Figure 12, the idea is moving the transversal barriers towards the cell ends, where the magnetic field is usually stronger. The central barrier is open at ends to allow the tapping crucible pipe placement. The velocity reduction at upstream has improved when compared with the previous result.

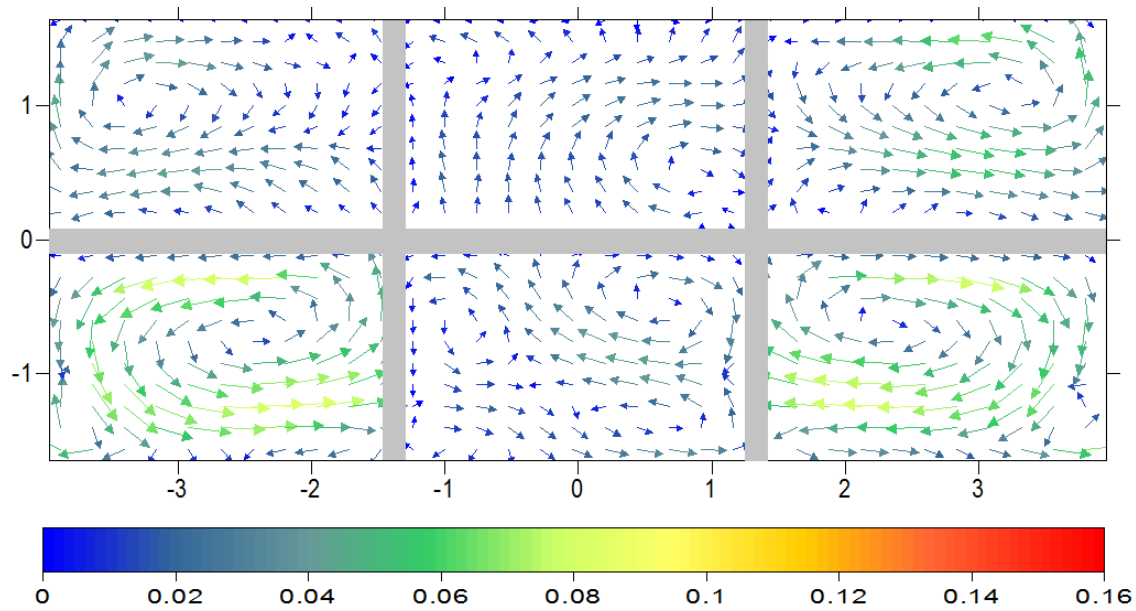

Figure 11: Metal velocities [m/s] calculated at the middle of the metal pad horizontal plane for case 4

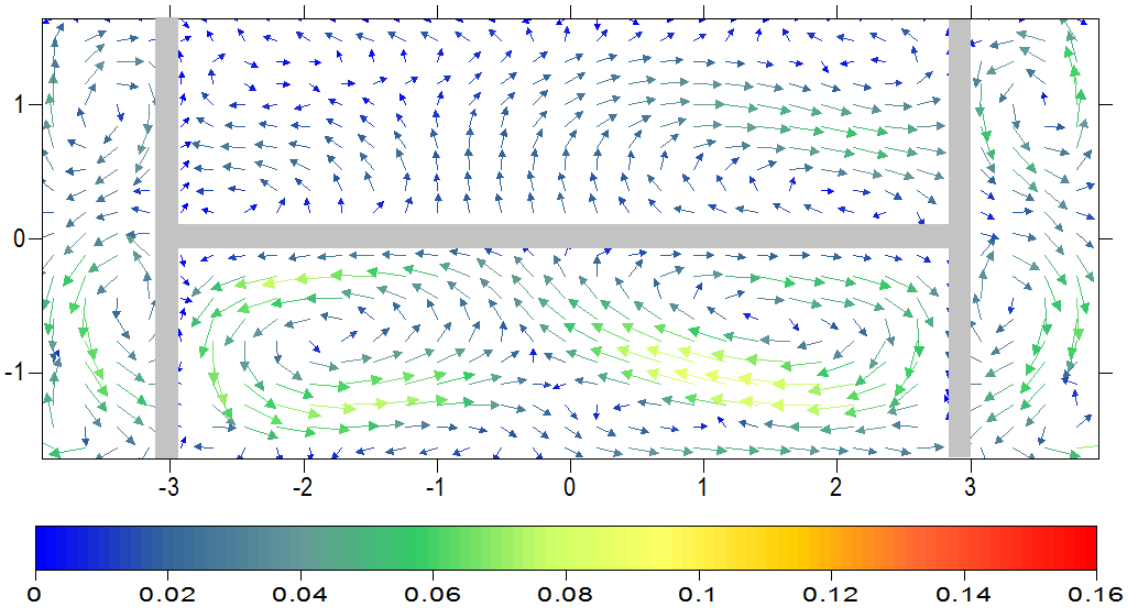

Figure 12: Metal velocities [m/s] calculated at the middle of the metal pad horizontal plane for case 5

The Figure 13 presents the metal velocity vectors for the structured cathode case. It is possible to verify an important decrease in velocity magnitude when compared with the traditional cell (Case 1). The two pools flow configuration is maintained however, the structures create the necessary friction to reduce the metal velocity.

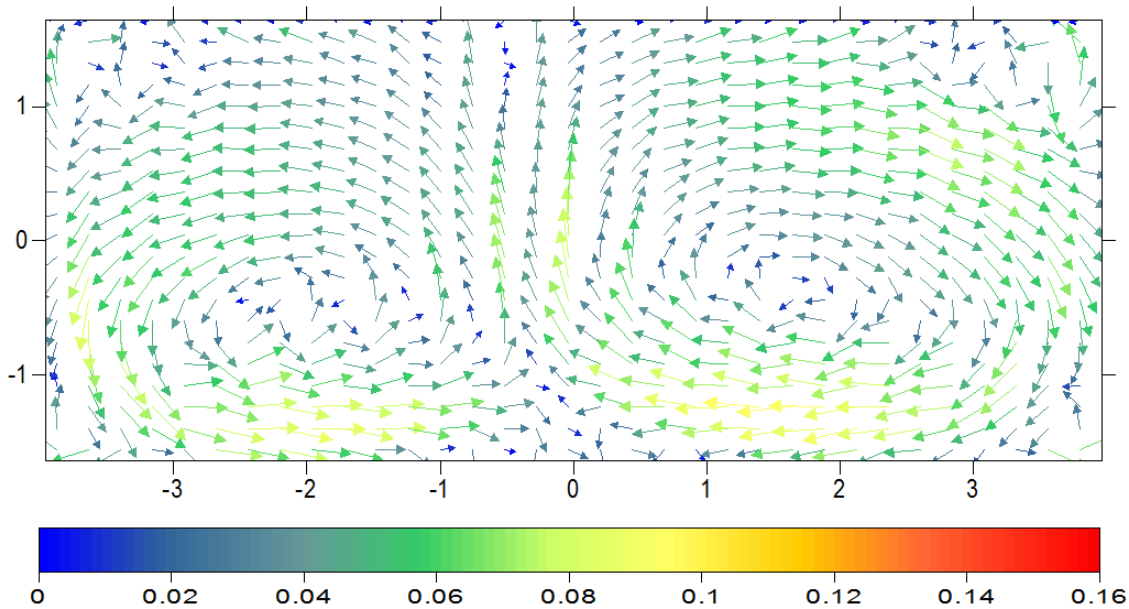

Figure 13: Metal velocities [m/s] calculated at the middle of the metal pad horizontal plane for case 6

The three-dimensionality of the flow can be observed in the Figure 14 and Figure 15. The vectors change the vertical direction near the barrier. Part of the flow is contained by the barrier and part of the flow is allowed to pass over the barrier but with reduced velocity.

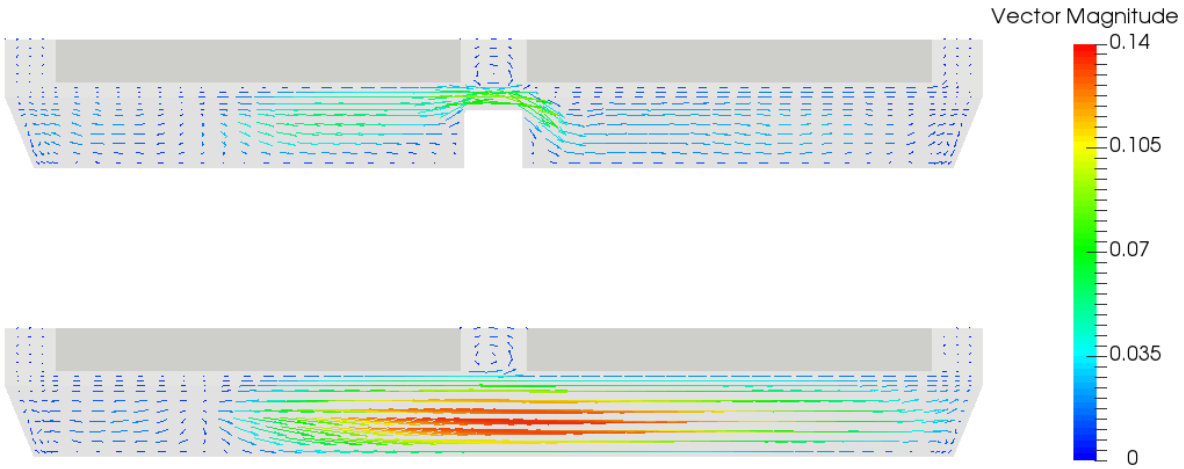

Figure 14: Metal velocities at the vertical cut of the cell. Above: Case 2 (central barrier). Below: Case 1 (traditional cell).

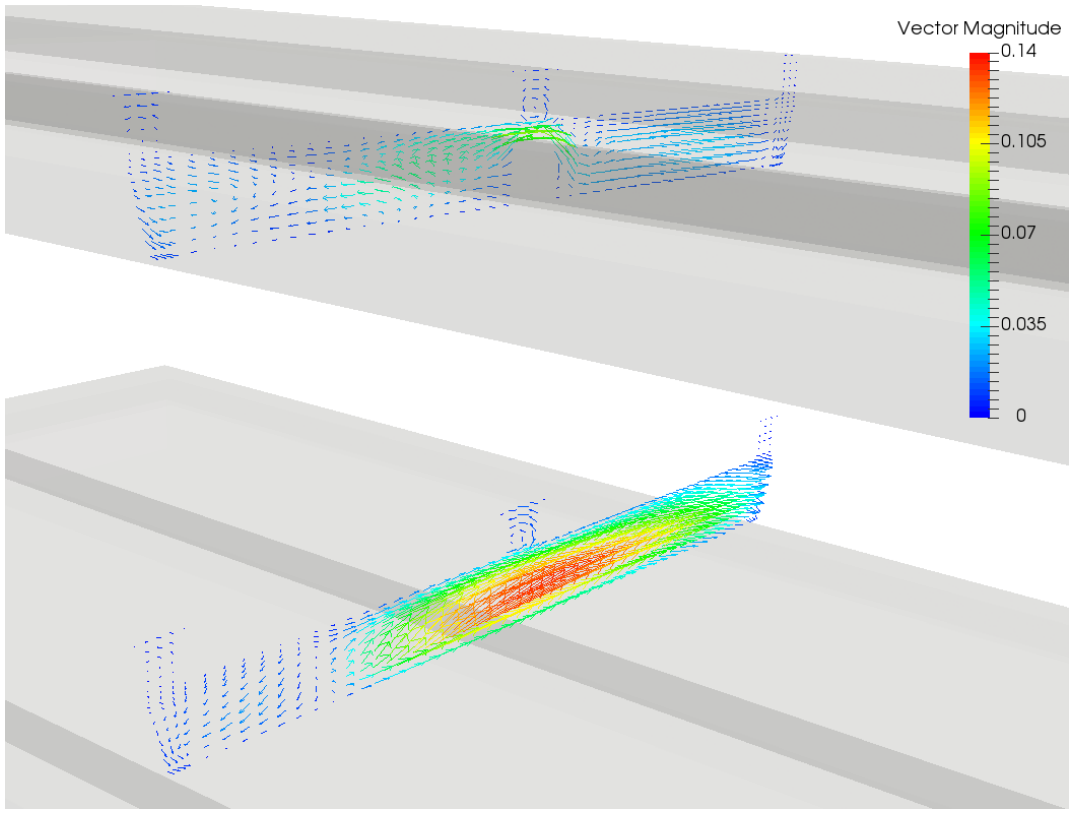

Figure 15: 3D view of metal velocities at the vertical cut of the cell. Above: Case 2 (central barrier). Below: Case 1 (traditional cell).

In the case of structured cathodes there is also important three-dimensional flow observed, for example in the Figure 16.

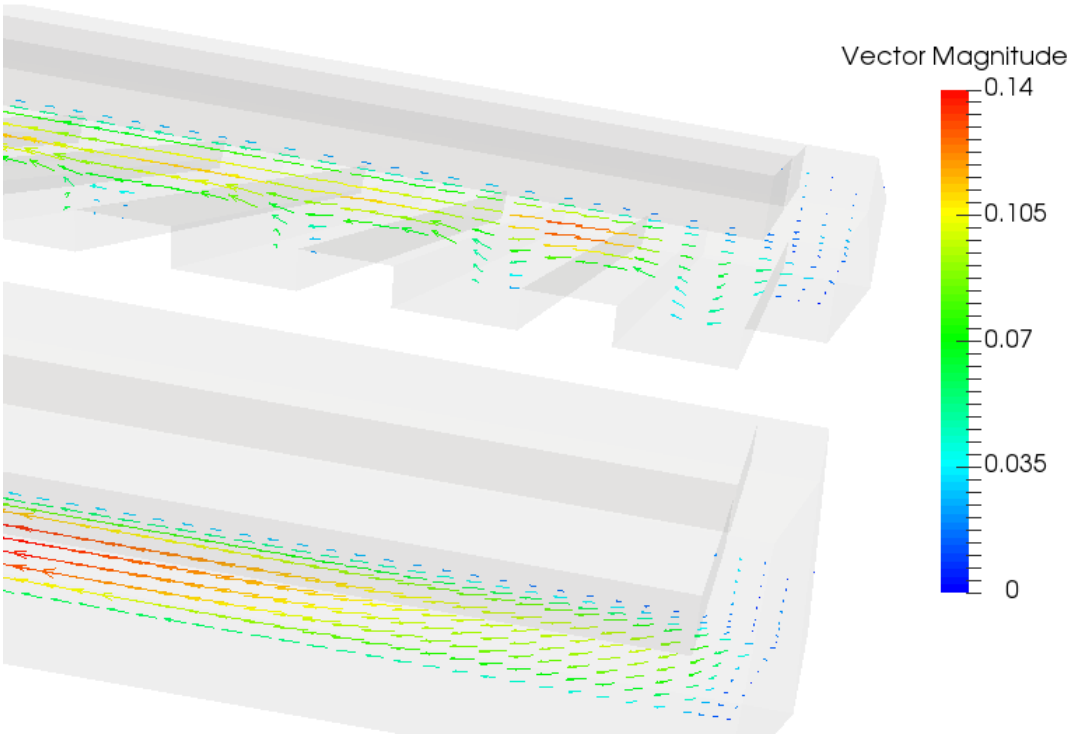

Figure 16: 3D view of metal velocities at the vertical cut of the cell. Above: Case 6 (structured cathodes). Below: Case 1 (traditional cell).

In the next pictures (Figure 17) the metal/bath interface deformation is shown for all cases. The contours present the vertical coordinates in units of [m], using the cathode top plane as reference. In the cases where a central channel barrier is used (cases 2, 3, 4, 5) the elevation becomes higher at upstream. In the presence of the barrier, the metal crossing from upstream to the downstream is restricted, increasing the interface deformation.

In the structured cathode case, the interface deformation becomes higher than the traditional cell. This can be explained by the velocity reduction caused by the structures. The kinetic energy is then stored as potential energy in the form of interface deformation.

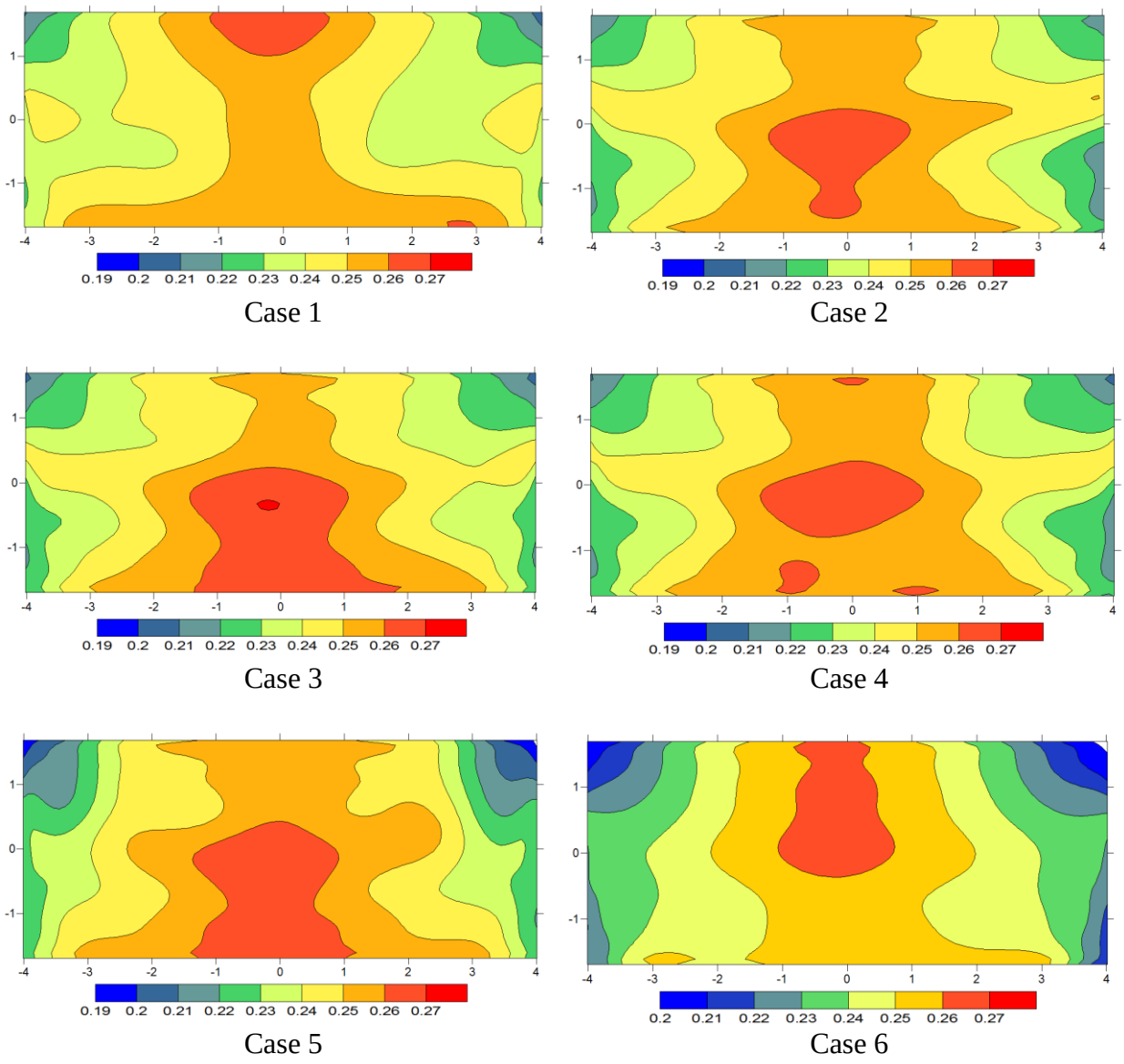

Figure 17: Metal/bath interface position [m] calculated for all cases

The results previously presented are summarized in Table 1. The central channel barrier (Case 2) reduced the metal velocity by more than 50 % on average, compared with the traditional cell (Case1). When the barrier has a tapping gap (Case 3), some localized high velocities appear. Even though, the average velocity is almost 50 % lower than the Case 1. When transversal barriers are installed in addition to the central channel barrier (Case 4 and Case 5), the velocities are further reduced. In Case 6, the benefit of structured cathodes in reducing metal velocity is confirmed, but less reduction is observed when compared with the barrier cases.

Table 1: Summary of steady state MHD flow for all calculated cases

	Average Velocity [cm/s]	Maximum Velocity [cm/s]	Total Interface Deformation (Max - Min) [cm]
Case 1	7.26	16.0	6.23
Case 2	3.15	9.8	5.68
Case 3	3.68	13.8	6.58
Case 4	2.56	8.4	6.04
Case 5	2.53	8.8	8.16
Case 6	4.36	10.5	7.17

Lower metal velocities potentially present a series of benefits to the cell such as:

- Less cathode top wearing is expected, increasing cell expected life;
- Reductions in cell sidewall heat transfer coefficients, which permits a greater ledge thickness. This protects the cell lining from thermal excursions also increasing cell expected life;
- Less metal re-dissolution into the bath due to the reduction of concentration boundary layer. This increases the process current efficiency.

Conclusions and Future Developments

Metal flow barriers appear to be an effective solution for improving the metal velocity pattern in aluminium reduction cells. Barriers are also expected to act as wave breaker and to improve cell MHD stability.

The MHD analysis of cells with metal barrier must be performed in three-dimensional models. The open source code Openfoam was successfully used for steady state calculation of fluid velocities and metal/bath interface at averaged steady state conditions.

The central channel barrier produces a radical change in the velocity pattern, breaking the two main pools present in the traditional cell. Transversal barriers can further improve the velocity reduction. Structured cathodes also have produced a general velocity reduction.

The metal/bath interface is not heavily affected by the barriers or structures. The tendency is to observe some increase in magnitude associated with the reduction of velocities.

The next logical step in the model development is to implement the cell instability model in Openfoam. Such a model must include the recalculation of electrical field inside Openfoam coupled with the wave movement. The Lorentz forces are then recalculated and applied at each time step of a transient calculation. It has been reported [6] that barriers have the ability to improve the cell MHD stability. Lower metal velocities and improved MHD stability may increase current efficiency or allow increasing the cell current.

References

[1] A. F. LaCamera, D. P. Ziegler, R. L. Kozarek, “Magnetohydrodynamics in the Hall-Heroult Process, an Overview”, *TMS Light Metals 1991*, pp 91-98.

[2] D. S. Severo, A. F. Schneider, E. C. V. Pinto, V. Gusberti, V. Potocnik, "Modeling Magnetohydrodynamics Of Aluminum Electrolysis Cells With ANSYS And CFX", *TMS Light Metals 2005*, 475-480.

[3] A. J. Gesing; E. W. Dewing, "Electrolytic Reduction Cells", *Patent US4495047 – 1985*.

[4] J. R. Humi; E. A. Hollingshead, T. G. Edgeworth, R. R. Sood; E. W. Dewing, C. J. Rogers, "Electrolytic Reduction Cells", *Patent US4505796 – 1985*.

[5] 高德金, 高伟, "Cathode lining with aluminum liquid magnetic rotational flow adjusting device", *Patent CN101649470B* - 2010.

[6] S. Renaudier, et al, "Alucell: A Unique Suite of Models to Optimize Pot Design and Performance", *TMS Light Metals 2018*, pp 541-549.

[7] Y. Ruan, E. A. Kuhn, J. S. Ubelhor, D. J. Duke "Apparatus and method for improving magneto-hydrodynamics stability and reducing energy consumption for aluminum reduction cells", *Patent US8795507B2 – 2014.*

[8] F. Naixiang, et al, "Energy Reduction Technology for Aluminum Electrolysis: Choice of the Cell Voltage", *TMS Light Metals 2013*, pp 549-552.

[9] D.S. Severo, V. Gusberti, A.F. Schneider, E.C. Pinto and V. Potocnik, "Comparison of various methods for modeling the metal-bath interface", *TMS Light Metals 2008*: 413-418, 2008.

[10] N. Feng et al., "Research and Application of Energy Saving Technology for Aluminum Reduction in China," *TMS Light Metals 2012*, 563-568.

[11] Y. Song, J. P. Peng, Y. W. Wang, Y. Z. Di, B. K. Li, N. X. Feng, "Magnetohydrodynamics Simulation of 300 kA Novel Cell for Aluminum Electrolysis", *Metalurgija* 55 (2016) 1, 22-24.

[12] Q. Wang, B. Li, Z. He, N. Feng, "Simulation of Magnetohydrodynamic Multiphase Flow Phenomena and Interface Fluctuation in Aluminum Electrolytic Cell with Innovative Cathode", *Metallurgical and Materials Transactions B - Volume 45B* - February 2014, pp 273-294.

[13] M. Dupuis, V. Bojarevics, "Influence of the Cathode Surface Geometry on the Metal Pad Current Density", *TMS Light Metals 2014*, pp 479-484.

[14] M. Dupuis, V. Bojarevics, "Non-Linear Stability Analysis of Cells Having Different Types of Cathode Surface Geometry", *TMS Light Metals 2015*, pp 821-826.

[15] M. Dupuis, M. Pagé, "Modeling Gravity Wave in 3D with Openfoam in an Aluminum Reduction Cell with Regular And Irregular Cathode Surfaces", *TMS Light Metals 2016*, pp 909-914.

[16] W. Ziqian, F. Naixiang, P. Jianping, W. Yaowu, Q. Xiquan, "Study of Surface Oscillation of Liquid Aluminum in 168kA Aluminum Reduction Cells with a New Type of Cathode Design", *TMS Light Metals 2010*, pp 485-488.

[17] V. Bojarevics and S. Sira, "MHD stability for irregular and disturbed aluminium reduction cells", *TMS Light Metals 2014*, 685-690.